

Physico - Chemical and Morphologic Structural Characterization of the Red Mud Obtained in the Romanian Alumina Plant

VASILE GEORGESCU^{1*}, MIHAELA BOMBOS^{2*}, CATALINA CALIN³, DORIN BOMBOS³

¹ Romanian Academy, Institute of Physical Chemistry Ilie Murgulescu, 202 Splaiul Independentei, 060021 Bucharest, Romania

² National Institute for Research Development for Chemistry and Petrochemistry- ICECHIM-Bucuresti, 202 Spl. Independetei, 060021, Bucharest, Romania

³ Petroleum-Gas University of Ploiesti, 39 Bucuresti Blvd, 100680, Ploiesti, Romania

The red mud is the main insoluble waste product from the manufacture of alumina by the Bayer hydrometallurgical process. Due to the accumulation in large quantities (0.8-1.2 metric tons waste / 1 metric ton of alumina) with a relatively high content of residual alkali and small granulation, it has been subject to many research activities, especially related to the techniques of neutralizing and enhancing its reuse under the form of various subproducts. This paper presents the results of the work undertaken by the collective of authors to evaluate the physico-chemical and morphological structure of red mud resulting from alumina production. The physico-chemical and morphological structure were analyzed using complex analytical methods (ICP-AES/OES, DCP, AAS, EDS-EDAX, SEM, DTAC, XRF, XRD, optical microscopy). The aim was to identify potentially active compounds for various environmental applications. To estimate the average chemical composition, by element, we used dispersion analysis, through the Gauss normal distribution method.

Keywords: red mud, materials characterization, alumina, waste product

Mainly, alumina (aluminium trioxide) is obtained by the hydrometallurgical Bayer process, through the chemical treatment of bauxite ore (most often of lateritic and / or karstic origin) with concentrated caustic soda solutions [1,2]. Manufacturing one metric ton of alumina requires 2-3 metric tons of bauxite and generates up to about 1.2 metric tons of solid waste in the form of red mud, accumulating annually worldwide million tons of waste. Bauxite ore is a mixture of hydrated aluminium oxides containing silica, iron oxides and other impurities. Processing conditions vary from one type of bauxite to another, mainly by applying different temperature and pressure levels in the process of solubilisation in alkaline medium.

The insoluble red mud waste resulting in the manufacture of alumina by the Bayer process, requires special attention, due to at least two of its main characteristics: high levels of alkali content as a result of the residual content of caustic soda, indicated by a high pH range in the field of 8-13; and the fine size of solid particles (of the order of microns up to 100 microns). The physical, chemical and mineralogical properties of red mud are determined primarily by the type of bauxite used as raw material, by the action of auxiliary components introduced in different phases of the alumina production process and by the processing conditions of bauxite in the hydrometallurgical Bayer process [3-8].

Compositionally, red mud is a complex material, including many compounds, some similar to those in the composition of the bauxite used as raw material, others resulted from the transformations taking place in various stages of the production process of alumina, as majority components like iron (goethite or hematite), aluminium (Gibbsite and Boehmite, resulted through an incomplete solubilisation of bauxite), alkalis and silica (as various desilication products, sodalite, cancrinite, resulted through the solubilisation and recrystallisation of silicoaluminates

in bauxite), but also a series of minority compounds (caolinite, anatase, rutile, calcite, hidrogarnet), and also various rare earth elements or other elements found as traces (Ba, Cr, Ga, Sn, V, Zr, Y, Ce, Gd, Sr, U, Th, etc.) [9,10].

Red mud is not recycled or used in industrial quantities, with small exceptions [11-30], and with a low economic efficiency, most of the efforts being focused on its neutralization [31]. The analysis of physico-chemical and mineralogical properties of red mud is a key step, very important to identify recycling solutions in the form of potentially active compounds for various environment applications or for the possible recovery of useful elements.

In Romania, a major aluminium producer in Central and Eastern Europe, important amounts of bauxite ore of varying origin were processed over the course of time, mainly in the form of imports, lateritic and karstic type bauxite (gibbsite, gibbsite - boehmite, boehmite and diasporite bauxites), the economic and market factors having usually an important role. Red mud waste resulting from the manufacture of alumina in conditions specific to the Romanian technologies, has been stored over time in the form of dumps, with storage on the ground in closed spaces.

This paper presents results of the research conducted by the collective of authors regarding the evaluation of the physical-chemical and morphological structure of the red mud resulting from alumina production in conditions specific to Romanian technologies, in order to find the main potentially active compounds for various environmental applications.

The physico-chemical and morphological structure were analyzed using complex analytical methods (ICP-AES/OES, DCP, AAS, EDS-EDAX, SEM, DTAC, XRF, XRD, optical microscopy). To estimate the average chemical composition, by element, we used dispersion analysis, through the Gauss normal distribution method.

* email: fgeorgescu@icf.ro; bombos.mm@gmail.com

Experimental part

Sampling

Red mud samples were taken inside the dumps along the accessible area. Where access was possible, multiple sub-samples were taken which were merged to form a single sample for that location. Red mud samples were collected as informative samples from predetermined locations using similar techniques. Overall, about 80 kg of red mud residue was collected and stored (stored) in plastic bags until the next day. In the laboratory, the samples of red mud were mixed thoroughly using a stainless steel spatula and transferred in polyethylene closed containers.

Analysis of majority elements and trace elements

For the analysis of majority elements and trace elements from the red mud, we used qualitative chemical analysis through atomic spectroscopy: atomic absorption spectroscopy (AAS/FAAS), atomic emission spectroscopy (ICP-AES/OES). A significant number of probes were analyzed in parallel. Dispersion analysis was used for assessing the estimated/average content of components, through the Gauss normal distribution method. For this purpose, the following values were calculated: the arithmetic mean (x_{med}), dispersion (s), standard error of the arithmetic mean. The analysis allows the determination of confidence intervals for the real values for chemical elements, for a given threshold of significance q (eq. 1):

$$X_{med} \pm tq \cdot s/n^{1/2} \quad (1)$$

Morphological and structural analysis

For the morphological and structural characterization of the red mud samples, imaging and quantitative compositional determinations were made, corresponding to the

X-ray emission spectrum through EDS-EDAX, SEM, XRF analysis, to investigate the distribution of surface properties on the initial mud samples and samples washed with distilled water and by XRD analysis and optical microscopy in polarized light to determine the mineralogical phase composition. Red mud samples collected from different areas of the landfills were processed and analyzed.

Two of the red mud samples were washed with distilled water in ratio (weight) mud: water of about 1:20, in stages of three washings/sample. The variation of the pH for the eluates and the necessary amount of water for reducing the pH of the samples to pH=8-8.5 (about 900 mL) were recorded. We observed that the filtrates present fine deposits over time. Initial mud samples and the washed samples were dried to constant weight in oven at about 100-105° C. The initial mud samples and the washed and dried ones were investigated in terms of image and composition through scanning electronic microscopy and EDS-EDAX (X-ray emission spectrum).

To make imaging determinations a Philips XL 30 ESEM TMP scanning electronic microscope was used, with a resolution of 3.5 nm at an accelerating voltage for the electron beam of 30 kV. Due to the fact that the probes are not conductive, in order to avoid the appearance of the surface electric charge phenomena, a water vapour environment was introduced in the microscope room with an average pressure of 0.7 Torr. Compo type images (differences in gray shades are also differences in the composition of the analysed surface) were obtained from 100, 500, 2000 and 5000x zoom levels, with a backscatter electron detector (BSE). The analysis for determining the chemical composition of samples was performed using an EDS-EDAX spectrometer with energy dispersion with a resolution of 128 eV. The data acquisition time was set to a

minimum of 35 sec, and the results were expressed in weight percents and atomic percents.

To determine the structural phase composition of the red mud, X-ray diffraction analysis (DRX) was used, and the data acquisition was performed on the BRUKER D8 ADVANCE diffractometer with the DIFFRAC^{PLUS} XRD COMMENDER (BRUKER AXS) software, through Bragg Brentano diffraction, θ - θ coupling, in vertical configuration, with Cu K α radiation; the materials were scanned in the 2θ domain Region 4 \div 74°, 2θ Step 0.02°, time (s)/step 4.5; scan mode: continuous; scan type: Locked Coupled; rotation speed (rot/min) 120, electronic removal of the CuK β component, with the SOL X detector. The phase analysis was performed using the EVA12 software - with the Search / Match Module and the ICDD PDF-2 Release 2006 database.

The red mud study by optical microscopy was conducted using a polarized light microscope, type AxioImager A1m, with image capture done by a Canon Power Shot A 640 digital camera, 10X digital zoom, and Axiovision Release 4.6.3 image processing software, on samples prepared through EpoThin resin embedding, according to the MICRO-A2-029 procedure.

Thermal analysis

The thermal analysis of red mud was performed with a SETSYS EVOLUTION device manufactured by the company SETARAM-FRANCE. The material was subjected to a controlled temperature program, a heating being carried out up to 1100°C at a heating rate of 10°C/min and a cooling to 500 at 10°C/min. The attached curves highlight a series of thermal effects related to mass variation. On the TG curve, several mass losses can be observed, due to changes also highlighted on the HEAT FLOW curve by endothermic effects.

Results and discussions

The physico-chemical analysis of the red mud, performed through complex ICP-AES/OES, DCP, AAS/FAAS techniques, has shown that, as expected, this has a complex composition (table 1 and table 2).

Mineralogical and structural analysis of the red mud made by X-ray diffraction (XRD) and optical microscopy also highlighted its complex composition. Mostly it is composed of iron oxides with earth aspect, probably hydrated, figure 1 (a,b), and contains between 18.97-20.01% iron, dispersed mainly in hematite Fe₂O₃ (30.4%) and goethite FeO(OH) (9.7%), and in small quantities in insoluble compounds - muscovite or in compounds generated through lying, hidrogarnet; it also contains between 7.1-7.7 % aluminium, dispersed in mainly diaspore AlO(OH) 7.6%, boehmite AlO(OH) 2.3%, gibbsite Al(OH)₃ 10.6%, but also in desilication compounds, in cancrinite Na₇²⁶²(CO₃)₃Al₆Si₆O₂₄ 7.8% and cancrisilite Na₇⁸⁶(Al₆Si₆O₂₄)(CO₃)(H₂O)₃ 11.4% (zeolitic compounds), or in compounds generated in bauxite solubilisation, hidrogarnet Ca₃AlFe(SiO₄)(OH)₈ 4.8%, as well as in insoluble compounds, muscovite (K,Na)(Al,Mg,Fe)₂(Si₃Al_{0.9})O₁₀(OH)₂ 1.9%, amesite (Mg₂Al)(AlSiO₃)(OH)₄ 2.1%, compounds that in addition to aluminium also include the following elements: 2.26-2.36 % Si; 2.68-2.91 % Na; 0.04-0.077 % K; 0.232-0.248% Mg; 3.348-3.697% Ca, (fig. 2 and table 3). A high humidity level of the red mud was found, between 31.38-32.73% and calcinations losses (1000°C) between 39.5-40.47%.

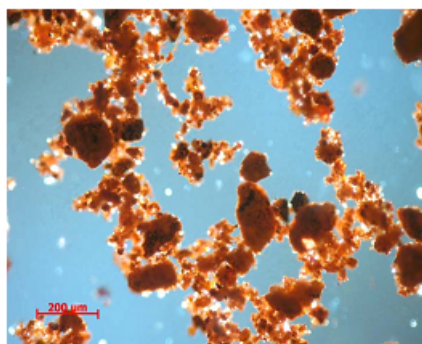
In the magnetic separation, optical microscopy found metallic iron and muschetovite, pseudomorph phase of magnetite Fe₃O₄, after hematite Fe₂O₃, (fig. 3:a,b). The muschetovitisation-martitisation processes are connected

Table 1
CHEMICAL COMPOSITION ON ELEMENTAL OF RED MUD (wt%)

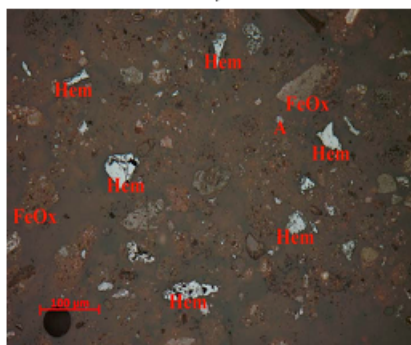
Element	Esantion							
	IA	IB	IC	ID	IE	IF	IG	II
	Element (%)							
Fe	1.941	17.86	17.47	17.67	21.01	19.31	23.71	19.46
Al	7.32	7.03	6.49	7.33	8.15	7.68	7.7	7.1
Si	2.25	2.32	2.62	2.31	2.24	2.17	2.02	2.58
Ti	2.73	2.23	2.16	2.75	2.46	3.11	2.34	2.23
Na	3.31	2.92	2.57	2.4	2.65	2.03	3.22	3.24
Ca	2.86	4.24	3.82	4.45	2.8	2.64	3.97	3.4
Ba	0.68	0.56	0.024	0.032	0.052	0.61	0.89	0.71
Mg	0.26	0.24	0.3	0.2	0.24	0.2	0.24	0.24
V	0.043	0.038	0.035	0.038	0.041	0.041	0.038	0.039
Zr	0.058	0.023	0.009	0.035	0.03	0.051	0.038	0.032
Cu	0.032	0.038	0.028	0.021	0.051	0.031	0.023	0.015
Pb	0.041	0.044	0.083	0.035	0.0720	0.056	0.048	0.053
K	0.026	0.024	0.020	0.078	0.024	0.033	0.0230	0.025
Zn	0.015	0.012	0.012	0.011	0.019	0.016	0.02	0.018
Ce	0.012	0.017	0.018	0.016	0.014	0.016	0.012	0.017
La	0.005	0.0061	0.0068	0.0053	0.0052	0.0049	0.0051	0.0057
Sc	0.0033	0.0038	0.0039	0.0039	0.0038	0.0025	0.003	0.0049
Ga	0.0028	0.0015	0.0016	0.002	0.003	0.0031	0.0028	0.0027
Y	0.0026	0.0033	0.0033	0.0033	0.0033	0.0025	0.0029	0.0028
As _{max}	0.002	0.002	0.002	0.002	0.002	0.002	0.002	0.002
Se _{max}	0.002	0.002	0.002	0.002	0.002	0.002	0.002	0.002
Th _{max}	0.002	0.002	0.002	0.002	0.002	0.002	0.002	0.002
U _{max}	0.002	0.002	0.002	0.002	0.002	0.002	0.002	0.002
Hg _{max}	0.001	0.001	0.001	0.001	0.001	0.001	0.001	0.001
C	0.75	0.9	0.91	0.81	0.86	0.85	1.01	0.75
H ₂ O	32.61	32.62	33.55	33.39	30.39	31.85	26.46	35.56
PC(1000°C)	42.12	40.02	42.93	40.23	38.66	37.34	37.34	41.24

Table 2
ESTIMATION OF AVERAGE CHEMICAL COMPOSITION ON ELEMENTS
(IN % WEIGHT; STATISTICAL ANALYSIS $\alpha=0.05$)

Element	Statistical analysis							
	Calculation of confidence interval							
	C _{med}	S(C-C _{med}) ²	S ²	S	SC _{med}	2SC _{med}	max	min
Fe	19.49	30.21	0.54	0.73	0.26	0.52	20.01	18.97
Al	7.35	1.78	0.03	0.18	0.06	0.13	7.48	7.22
Si	2.31	0.28	0.01	0.07	0.03	0.05	2.36	2.26
Ti	2.50	0.78	0.01	0.12	0.04	0.08	2.58	2.42
Na	2.79	1.47	0.03	0.16	0.06	0.11	2.91	2.68
Ca	3.523	3.4186	0.061	0.25	0.09	0.175	3.697	3.348
Ba	0.445	0.8662	0.015	0.12	0.04	0.088	0.533	0.357
Mg	0.240	0.0072	0.00013	0.01	0.004	0.008	0.248	0.232
V	0.039	0.00004	7.6E-07	0.001	0.0003	0.0006	0.040	0.039
Zr	0.035	0.0011	1.9E-05	0.004	0.0016	0.0031	0.038	0.031
Cu	0.030	0.0009	1.54E-05	0.004	0.0014	0.0028	0.033	0.027
Pb	0.054	0.0017	2.98E-05	0.005	0.0019	0.0039	0.058	0.050
K	0.059	0.0390	0.000697	0.026	0.0093	0.0187	0.077	0.040
Zn	0.015	0.0001	1.5E-06	0.001	0.0004	0.0009	0.016	0.015
Ce	0.015	2.69375E-05	4.81E-07	0.000694	0.0002	0.0005	0.016	0.015
La	0.006	2.72609E-06	4.87E-08	0.000221	7.8E-05	0.0002	0.0057	0.0054
Sc	0.004	3.48484E-06	6.22E-08	0.0002	0.0001	0.0002	0.0038	0.0035
Ga	0.002	2.72734E-06	4.87E-08	0.0002	0.0001	0.0002	0.0026	0.0023
Y	0.003	0.00000066	1.18E-08	0.000109	3.84E-05	0.0001	0.0031	0.0029
As _{max}	0.002	0	0	0	0	0	0.0020	0.0020
Se _{max}	0.002	0	0	0	0	0	0.0020	0.0020
Th _{max}	0.002	0	0	0	0	0	0.0020	0.0020
U _{max}	0.002	0	0	0	0	0	0.0020	0.0020
Hg _{max}	0.001	0	0	0	0	0	0.0010	0.0010
C	0.855	0.042	0.00075	0.0274	0.0097	0.0194	0.874	0.836
H ₂ O	32.054	50.74	0.906	0.952	0.337	0.673	32.73	31.38
PC(1000°C)	39.985	26.06	0.465	0.682	0.241	0.482	40.47	39.50



a)



b)

Fig. 1. Red mud sample, IA, parallel nicoles, a) transmission light; b) reflected light (FeOx-iron oxides with earth aspects, Hem-hematite, A -anatase, TiO₂)

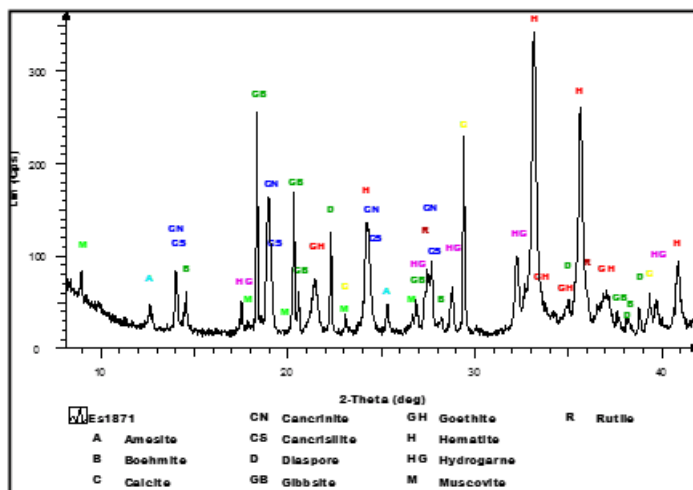
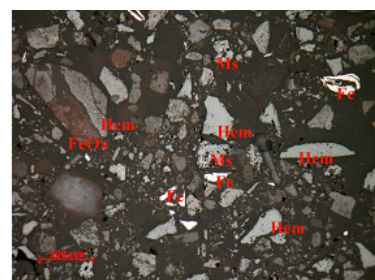
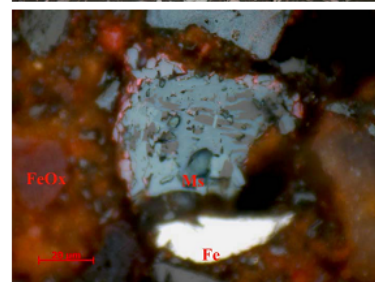


Fig. 2. Graphic presentation of X-ray analysis (XRD) for red mud sample drayed at 105° for 2h, representative details of diagram



a)

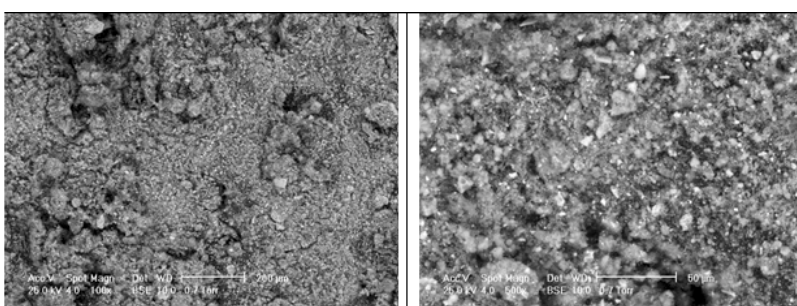


b)

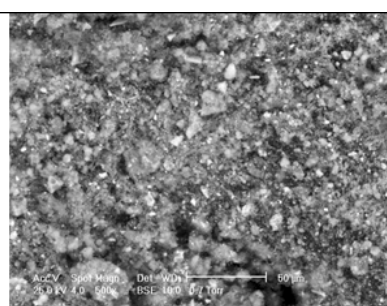
Fig. 3. Magnetic separation fraction (sample IA), nicoles parallel, a) reflected light; b) reflected light, immersion in cedru oil FeOx-iron oxides with earth aspect, Hem-hematite, Ms-muschetovite, Fe- ferric metal.

Table 3
SEMICANTITATIVE PHASE ANALYSIS, DRAYED RED MUD SAMPLE (105°C, 2H)

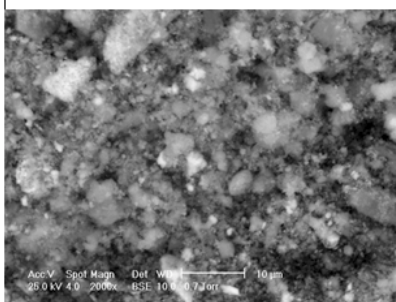
Compound Name	Formula	S-Q (%ms.)	PDF Reference
Hematite	Fe ₂ O ₃	30.4	01-087-1164 (*)
Goethite	FeO(OH)	9.7	01-081-0464 (I)
Diaspore	AlO(OH)	7.6	01-084-0175 (*)
Boehmite	Al(OH) ₃	2.3	01-083-1505 (I)
Gibbsite	Al(OH) ₃	10.6	01-074-1775 (I)
Calcite	CaCO ₃	9.2	01-071-3699 (*)
Rutile	TiO ₂	2.3	01-070-7347 (*)
Cancrinite	Na _{7.262} (CO ₃) _{0.932} Al ₆ Si ₆ O ₂₄	7.8	01-089-8592 (*)
Cancrinite	Na _{7.86} (Al ₆ Si ₆ O ₂₄)(CO ₃)(H ₂ O) _{3.3}	11.4	01-089-8047 (N)
Hydrogarnet	Ca ₃ AlFe(SiO ₄)(OH) ₈	4.8	00-032-0147 (C)
Muscovite	(K,Na)(Al,Mg,Fe) ₂ (Si _{3.1} Al _{0.9})O ₁₀ (OH) ₂	1.9	00-007-0042 (I)
Amesite	(Mg ₂ Al)(AlSi ₅ O) ₄ (OH) ₄	2.1	01-087-2057 (*)



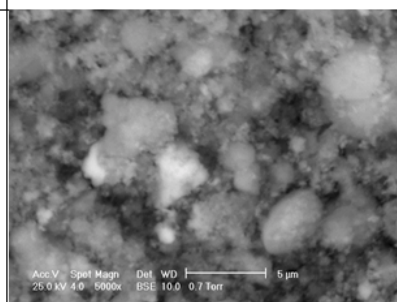
a) magnification x 100.



b) magnification x 500.



c) magnification x 2000.



d) magnification x 5000.

Fig. 4. SEM Micrographs, showed shape and surface of red mud particles: irregular particles with variable size (2 - 100μm)

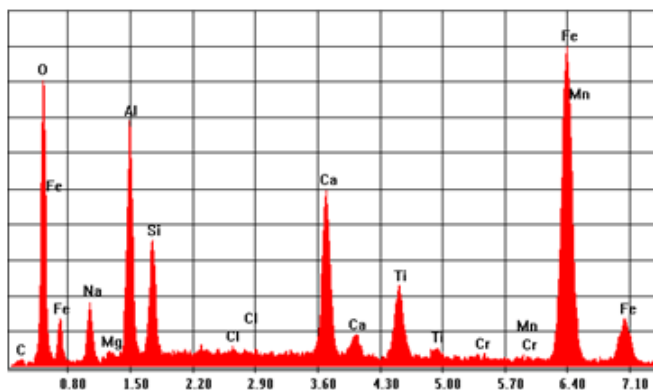


Fig. 5. Emission spectra of the X-ray radiations obtained in EDS-EDAX analysis, red mud sample, IA probe, showed presence of O₂, Fe, Na, Al, Ca, Mg, Si, Ti, Cr, Mn, Cl

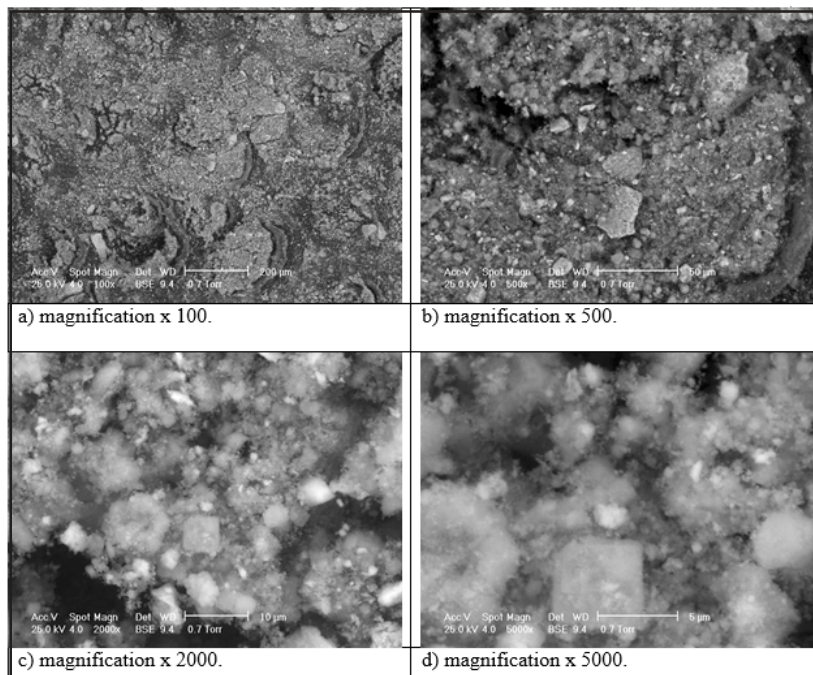


Fig. 6. SEM Micrographs, showed shape and surface of washed red mud particles: irregular particles with variable size (2 - 100µm)

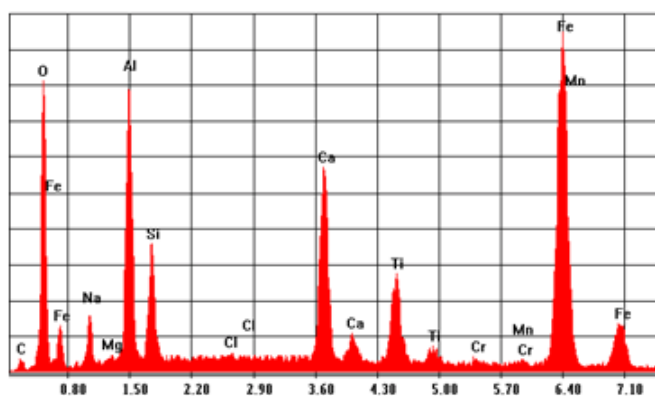


Fig. 7. Emission spectra of the X-ray radiations obtained in EDS-EDAX analysis, washed red mud sample, IA probe, showed presence of O₂, Fe, Na, Al, Ca, Mg, Si, Ti, Cr, Mn, Cl

to the change in the oxidation and reduction potential after the deposit of these materials from hydrothermal solutions.

We have also shown that the analysed red mud contains minor components and traces of Ba, Mg, V, Ti, Zr, Cu, Pb, Zn, Ce, La, Sc, Ga, Y, (table 1 and table 2). As far as the content of As, Se, Th, U, Hg is concerned, these elements have a concentration in the analyzed red mud under the detection limit of the devices used for chemical analysis.

The morphological and structural study results, obtained through imaging and quantitative composition corresponding to the X-ray emission spectrum from EDS-EDAX, SEM analysis, shown in figure 4(a,b,c,d) and figure 5, respectively figure 6(a,b,c,d) and figure 7, and through XRF analysis, conducted to investigate the distribution of

surface properties of the initial mud samples and those washed with distilled water, support the presented results obtained by X-ray diffraction and optical microscopy. The SEM images recorded at several resolutions of the samples of red mud present a non-uniform structure with agglomerations of crystallites in different areas and different dimensions, specific to the mixtures of oxides with a majority phase. After washing with distilled water the agglomerations of crystallites are preserved. It was also found that by washing the mud samples at neutral pH (pH 8-8.5), compounds like: Gd₂O₃, Ga₂O₃, and Sc₂O₃, are not found any more in the washed mud sample.

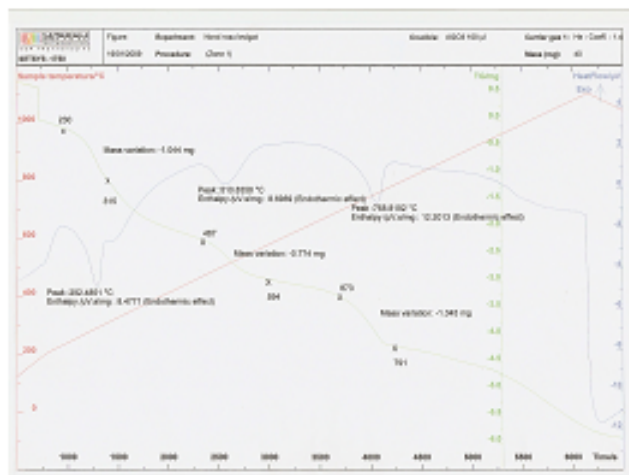


Fig. 8. Thermal DTAC curves of red sample, probe IA

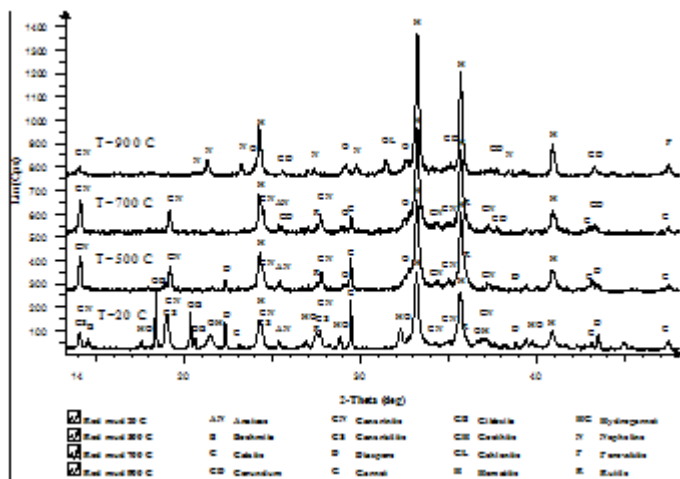


Fig. 9. Red mud thermal transformations, showed in X-ray analysis (XRD) (representative details of diagrams)

The thermal analysis (DTAC) indicates important mass losses in the domain 20-300°C (approximately 30%) and losses on the order of 1.5-4% on the domains 300-500°C, 500-700°C, 700-900°C. The thermal differential analysis (DTAC) for the IA sample highlighted four peaks (100°C, 292°C, 510°C, 768°C) corresponding to endothermic effects due to losses of physically retained water and water included in aluminosilicates of zeolite type and also due to phase changes of aluminium and iron compounds: gibbsite transforms in up to corundum; goethite up to hematite, (figs. 8-9).

Conclusions

The physico-chemical, morphological and structural analysis of red mud samples revealed a complex composition, mostly formed by iron oxide with earth aspect (dispersed mainly in hematite) and goethite FeO(OH) and in small quantities in insoluble compounds of muscovite type or in compounds generated in the solubilisation of hidrogarnet type, aluminium oxides dispersed mainly in diaspore, boehmite, and gibbsite, but also in desilication compounds in the composition of cancrinite and cancrisilite (compounds of zeolite type) or in compounds generated in the solubilisation of hidrogarnet type, as well as insoluble compounds as muscovite and amesite. In small quantities on the order of percents, the following elements are found: Si, Na, K, Mg and Ca. In the magnetic separation, optical microscopy found metallic iron and muschetovite, magnetite pseudomorph phase, after hematite. Also, the analyzed red mud contains minor components and traces of Ba, Mg, V, Ti, Zr, Cu, Pb, Zn, Ce, La, Sc, Ga, Y. As far as the As, Se, Th, U, Hg content is concerned, these elements have a concentration in the analyzed red mud under the detection limit of the devices used for chemical analysis. A high humidity level of the red mud was found, between 31-33% and calcinations losses (1000°C) between 39-42%.

References

- ZHUROV,V.V., BOGATYREV, B.,DEMINA,L., MATVEYEVA,V, Int. Geo. Rev., **26**, no.7, 1984, p.816;
- BOGATYREV,B.A.,ZHUROV,V.V., TSEKHOVSKY,YU.G., Lit. Min. Res., **44**, no.2, 2009, p.135;
- ZHENG, K., GERSON, A.R.,ADDAI-MENSAH, J., SMART,R., J. Cryst. Growth, **171**, no.1-2, 1997, p.197;
- GERSON, A.R., ZHENG,K., J. Cryst. Growth, **171**, no. 1-2, 1997, p.209;
- BARNES,M.C., ADDAI-MENSAH, J., GERSON,A.R., Microporous and Mesoporous Materials, **31**, no. 3, 1999, p.287;
- BARNES, M.C., ADDAI-MENSAH, J.,GERSON, A.R., Colloid and Surfaces, A: Physicochemical and Engineering Aspects, **147**, no.3, 1999,p.283;

- BARNES,M.C.,ADDAI-MENSAH, J., GERSON,A.R., Microporous and Mesoporous Materials, **31**, no.3, 1999, p. 303;
- BARNES,M.C., ADDAI-MENSAH, J.,GERSON,A.R., Colloid and Surfaces, A: Physicochemical and Engineering Aspects, **157**, no.1-3, 1999, p.101;
- PASCUAL, J., CORPAS, F.A., LOPEZ-BECEIRO, J., BENITEZ-GUERRERO, M., ARTIAGA,R., Journal of Thermal Analysis and Calorimetry, **96**, no.2, 2009, p.407;
- ATASOY, A.,Journal of Thermal Analysis and Calorimetry, **90**, no.1, 2007, p. 153;
- NICULESCU, M., IONITA, A.D., FILIPESCU, L., Rev. Chim. (Bucharest), **60**, no.11, 2009, p. 1189;
- CASTALDI, P., SILVETTI, M., SANTONA, L., ENZO, S., MELIS, P., Clays and Clay Minerals, **56**, no.4, 2008, p.461;
- PALMER, S.J., REDDY, B.J., FROST, R.L., Spectrochimica Acta Part A: Molecular and Biomolecular Spectroscopy, **71**, no.5, 2009, p.1814;
- WAGH, A.S., PINNOCK, W.R.,Economic Geology, **82**, no.3, 1987, p. 757;
- RESSWELL, P.J., GRAYSON, J.L., SMITH, A.H., U.S.A. Pat., no. 4,668,485, Appl., no. 807,319;
- SANTONA, L., CASTALDI, P., MELIS, P., J. Haz. Mat., **136**, no. 2, 2006, p.32;
- ZHANG, P.C., SPARKS, D.L., Environ. Sci. Technol., **24**, no. 12, 1990, p. 1848;
- SYLVESTER, P., WESTERHOFF, P., MOOLLER, T., BADRUZZAMAN, M., BOYD, O., Environ. Eng. Sci., **24**, no. 1, p. 104;
- LIU, W., YANG, J., XIAO, B., J. Haz. Mat., **161**, no. 1, 2009, p.474;
- YANG, J., ZHANG, D., HOU, J., HE, B., XIAO, B., Ceram. Int., **34**, no. 1, 2008, p.125;
- KHAITAN, S., DZOMBAK, D.A., LOWRY, G.V., Env. Eng. Sci., **26**, no. 2, 2009, p. 431;
- SGLAVO, VM., MAURINA, S., CONCI, A., SALVIATI, A., CARTURAN, G., COCCO, G., J. Eur. Cer. Soc., **20**, no. 3, 2000, p. 245;
- KAVAS, T., Build. Env., **41**, no. 12, 2006, p.1779;
- BISWAS, S., SATAPATHY, A., Mat. Design, **30**, no. 8, 2009, p. 2841;
- JUSTIZ-SMITH, N., BUCHANAN, V.E., OLIVER, G., Mat. Sci. Eng.A., **420**, no. 1-2, 2006, p.250;
- SORUH, S., ERGUN, O.N., J. Haz. Mat., **173**, no. 1-3, 2010, p. 468;
- PALMER, S.J., FROST, R.L., NGUYEN, T., Coord. Chem. Rev., **253**, no. 1-2, 2009, p.250;
- PEAK, D., SPARKS, D.L., Environ. Sci. Technol., **36**, no. 7, 2002, p. 1460;
- APPELO, C.A.J., VAN DER WEIDEN, M.J.J., TOURNASSAT, C., CHARLET, L., Environ. Sci. Technol., **36**, no. 14, 2002, p. 3096;
- ION, C.S., BOMBOS, M., VASILIEVICI, G., PANAITESCU, C., DRAGOMIR, R., Rev. Chim. (Bucharest), **68**, no. 4, 2017, p.732;
- NICULESCU, M., IONITA, A.D., FILIPESCU, L., Rev. Chim. (Bucharest), **60**, no. 11, 2009, p. 1189.

Manuscript received: 7.03.2018